JOURNAL OF APPLIED ELECTROCHEMISTRY 5 (1975) 343–349

The effect of silicate ion on the anodic behaviour of zinc in concentrated alkali

R. W. LEWIS, J. TURNER

Timex Corporation, Stephenson Estate, Washington, Co. Durham, U.K.

Received 26 October 1974; revised 26 February 1975; accepted 20 March 1975

The anodic behaviour of zinc in 8 M NaOH/1 M $Na_2Zn(OH)_4$, containing 0.1, 1 and 10 v/o sodium silicate solution, has been studied under quiescent conditions at ambient temperature using cyclic linear sweep voltammetry in conjunction with darkfield illumination optical photo-microscopy.

Results, together with measurements of the double layer capacitance of the zinc/alkali interphase as a function of potential, suggest the presence of a surface film of silicate which induces early passivation in the anodic potential excursion.

1. Introduction

The behaviour of silicate ion as an extender for the Zn/KOH system has been the subject of several papers in the literature [1–3], and is attributed to its ability to stabilise micelles of ZnO or $Zn(OH)_2$ by providing a better developed hydration sheath. Marshall *et al.* [4] have demonstrated its beneficial effect on the anodic behaviour of zinc in flowing KOH at current densities below i_l, the limiting current density for passivation. The following work investigates the influence of silicate additive on the passivation of zinc in concentrated sodium hydroxide solution under quiescent conditions.

2. Experimental

2.1. Cell design

Two cells were employed in the investigation: a P.T.F.E./pyrex three electrode cell designed for microscopic viewing to a specification published by R.W. Powers [5], and a pyrex cell, shown in Fig. 1, for the impedance measurements. The P.T.F.E. cell has been described in detail by Powers who has demonstrated its use in electrochemical studies on zinc [6, 7]. The circular viewing window was cut from a No. 3 microscope glass cover-slip (Chance Propper Ltd.) mounted on the end of a pyrex tube by R.T.V. silicone rubber adhesive (General Electric). The adhesive was

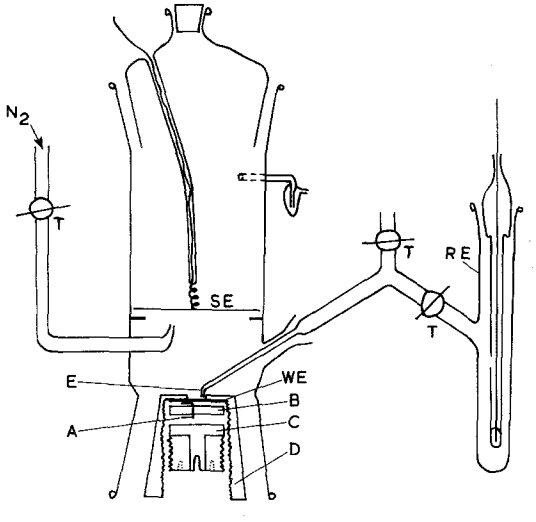

Fig. 1. Impedance cell. WE – working electrode; SE – subsidiary electrode; RE – Hg/HgO reference electrode; A – gold foil; B – silicone rubber washer; C – copper contact; D – PTFE electrode mounting; E – Luggin capillary; T – PTFE taps.

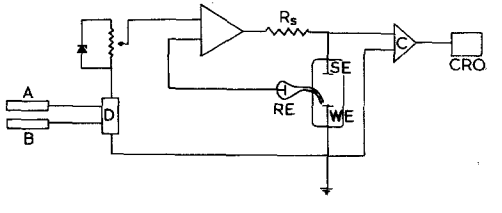

Fig. 2. Circuit diagram for impedance measurements. A – function generator; B – linear sweep unit; C – pre-amp; D – adder; CRO – oscilloscope.

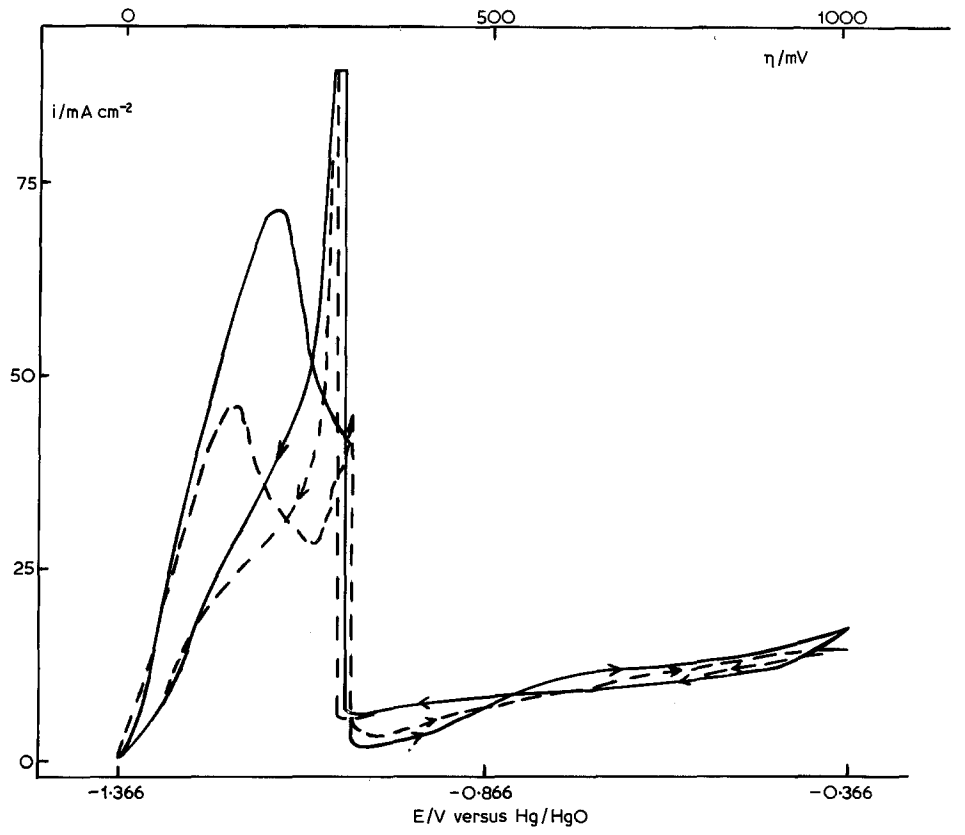

Fig. 3. Cyclic voltammograms for 8 M NaOH/1 M $Na_2Zn(OH)_4$. —— 1·67 mV s^{-1} ---- 0·83 mV s^{-1}.

cured for 24 h in an oven at 50°C and then exposed to electrolyte for 24 h before use. The cell possessed a gas lift-pump to provide conditions of enforced convection.

The subsidiary electrode of the impedance cell consisted of a circular disc of Pt foil whose overall area (31·8 cm^2) far exceeded that of the working electrode (0·28 cm^2).

2.2. *Techniques and equipment*

The method of determining the double-layer capacitance (C_{dl}) was that due to McMullen and Hackerman [8] who used it to study the surface roughness of various metal electrodes in aqueous solution. A periodic square wave pulse is applied to the interphase and the capacitive charging profile observed. At high frequencies (~500 Hz), $t \ll RC$–where t is the pulse width and RC the time constant of the circuit comprising electrochemical cell and current sensing resistor–and it is possible to observe the double layer relaxation free of Faradaic contributions.

A circuit diagram for the technique is given in Fig. 2. A chemical electronics TR40/3A potentiostat and linear sweep unit were used in conjunction with a Wavetek 144 function generator, which provided the low amplitude square wave (≤5 mV). Charging profiles were recorded on a Solartron CD1400 oscilloscope fitted with a CX1879 camera and film module.

In the linear potential scan experiments, current-voltage curves were recorded on a Bryans X-Y plotter type 26000 A4, and a Leitz Metallux metallurgical microscope with x 10 darkfield objective gave a magnification of x 100 for the optical work. Micrographs were taken with a CB100 Polaroid attachment camera and film pack.

2.3. *Preparation*

The electrolyte solution was made up from analaR grade zinc oxide and sodium hydroxide (BDH Ltd.) using triply distilled water, and the laboratory reagent grade sodium silicate solution, density 1·5 g cm^{-3}, was provided by Hopkin and Williams

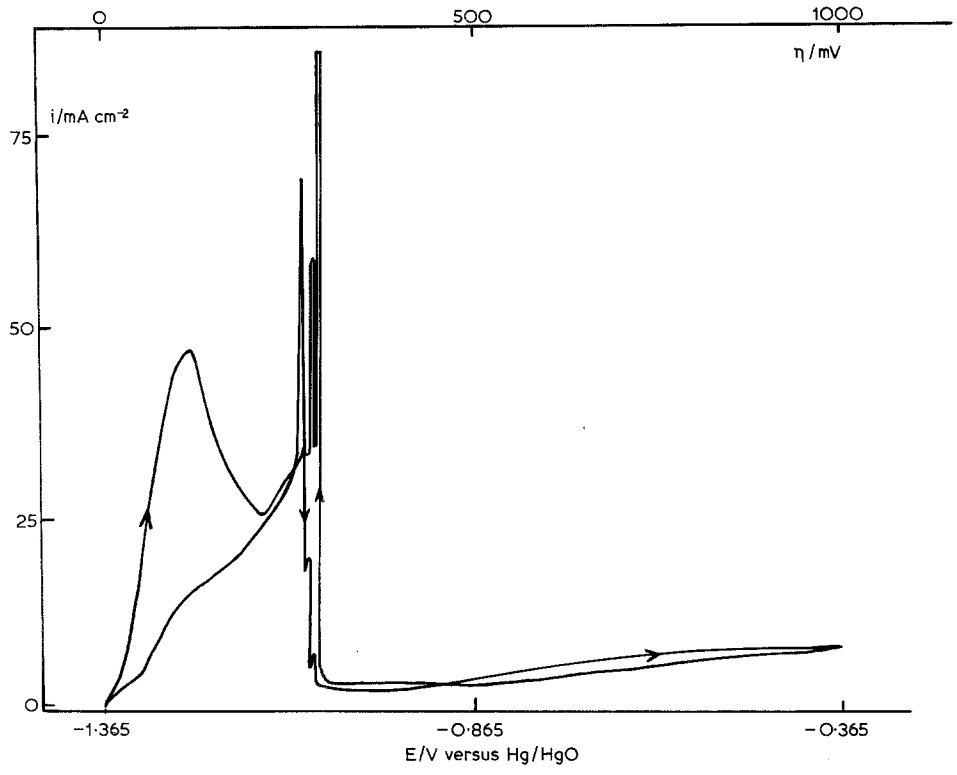

Fig. 4. Cyclic voltammogram for 8 M NaOH/1 M $Na_2Zn(OH)_4$/1 v/o Na_2SiO_3. Sweep rate: 0·83 mVs^{-1}.

Limited. The zinc foil, thickness 0·15 mm, purity 99·995 + % (Goodfellow Metals Ltd.) was blanked into the form of 1 in diameter discs, which were given a one second dip in 3 N HNO_3 followed by thorough washing in running triply distilled water prior to incorporation into the cell. The latter was filled immediately with electrolyte previously deoxygenated by passage of nitrogen (BOC Ltd., white spot grade). The zinc pre-treatment and filling procedure were conducted under a nitrogen atmosphere in a glove box.

3. Results and discussion

Figs. 3 and 4 show anodic cyclic current potential curves for zinc in the absence and presence of silicate ion respectively. The passivation can be seen to occur in two distinct stages: firstly, partial blocking of the electrode surface by anodic product resulting in a reduction in current density, followed by a sharp active-passive transition. The film (Type I) corresponding to the first peak is believed to form by a dissolution-precipitation mechanism, whereas the active-passive transition results from the formation of a compact low porosity zinc oxide film (Type II) directly on the zinc surface [6]. The sharp reverse peak arises from reduction of the Type II film which, being in intimate contact with the metal, is readily available for reduction; in contrast, a considerable amount of the Type I film still remains after completion of the anodic excursion.

Fig. 5 displays the colour changes accompanying the respective anodic and cathodic sweeps. The observed darkening of the oxide coating with continued increase in potential after passivation is attributed to an increase in its metallic zinc content [9, 10]. Such colour changes were observed both in the presence and absence of silicate.

Results for the investigation are summarised in Table 1. It is clear that the presence of silicate causes both the Type I and Type II films to occur earlier in the anodic excursion. Furthermore, the formation and reduction of the Type II film occurs in stages. Fig. 6 refers to conditions of enforced convection, such experiments being performed to obtain micrographs of the Type II film. Representative micrographs, which relate to the particular

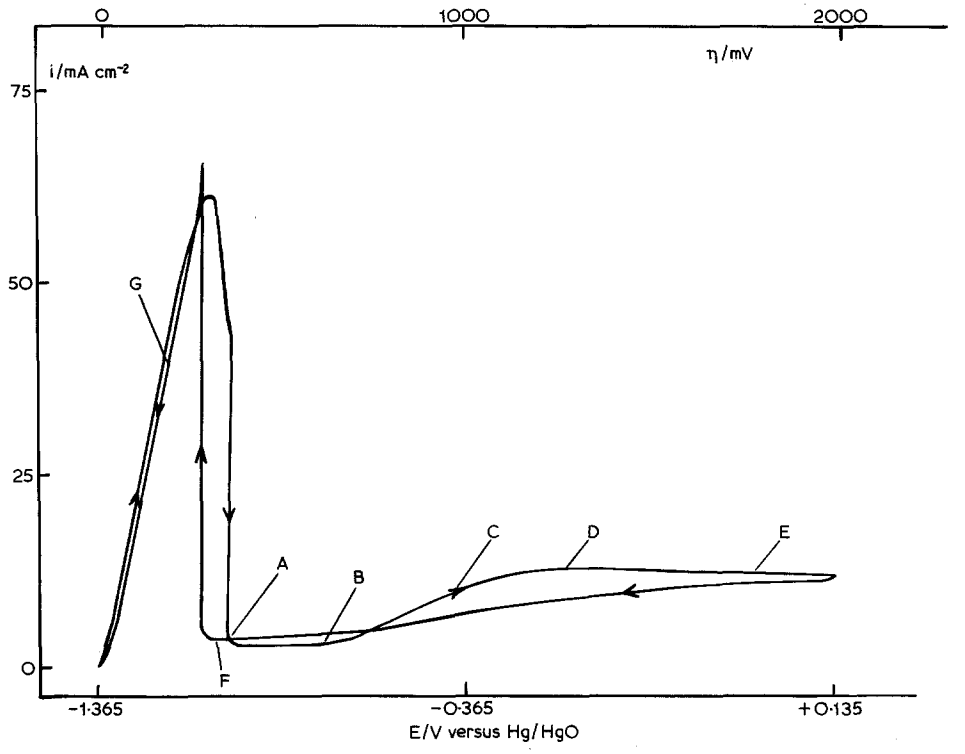

Fig. 5. Cyclic voltammogram for 8 M NaOH/1 M $Na_2Zn(OH)_4$. Sweep rate: 0·83 mV s^{-1}. A – white; B – bronze; C – light brown; D – chocolate brown; E – blue/black; F – light brown; G – light bronze/gold.

Table 1.

Additive	*Peak I*	*Peak(s) II*	*Reverse Peak (s)*	*Sweep Rate/mV s^{-1}*
None	222 ± 4	317 ± 6	309 ± 7	1·67
None	172 ± 5	314 ± 8	305 ± 6	0·83
0·1 v/o	99 ± 3	261 ± 2 270 ± 2 276 ± 4	292 ± 4 253 ± 4	1·67
0·1 v/o	94 ± 3	269 ± 7 275 ± 6 282 ± 6	293 ± 4 265 ± 4	0·83
1 v/o	100 ± 3	273 ± 5 270 ± 6 280 ± 5	280 ± 4 263 ± 2 254 ± 6	1·67
1 v/o	92 ± 3	268 ± 4 274 ± 5 282 ± 5	287 ± 4 280 ± 4 272 ± 6 267 ± 5	0·83
10 v/o	114 ± 2	262 ± 2 277 ± 2	314 ± 4 294 ± 6 263 ± 3	1·67
10 v/o	100 ± 3	260 ± 4 273 ± 2	310 ± 5 292 ± 7 268 ± 6	0·83

N.B. all potentials quoted in mV on overpotential scale.

regions of the voltammograms indicated are presented in Figs. 7 and 8. The cathodic displacement of the peaks does not vary significantly at constant sweep rate with silicate concentration over the range studied. The sweep rate dependence of the current maxima for peak I (i_m), is given in Fig. 9.

Fig. 10 shows the dependence of the double-layer capacitance on electrode potential, from which it can be seen that C_{dl} is substantially lowered in the presence of silicate, indicating specific adsorption of silicate ions.†

A theoretical interpretation of the influence which such an adsorbed film would have on the critical free energy (ΔG^*) for nucleation of zinc

† It is extremely unlikely that any diffuse layer effects will contribute to C_{dl} because of the high concentration of OH^- and thus we may assume that essentially inner layer capacities are measured. The C_{dl}/E curves do not refute this assumption, as evidenced by the absence of a sharp minimum and the virtual potential independence of C_{dl} at potentials where no Faradaic current flows, although the potential range studied is not sufficiently extensive to be conclusive.

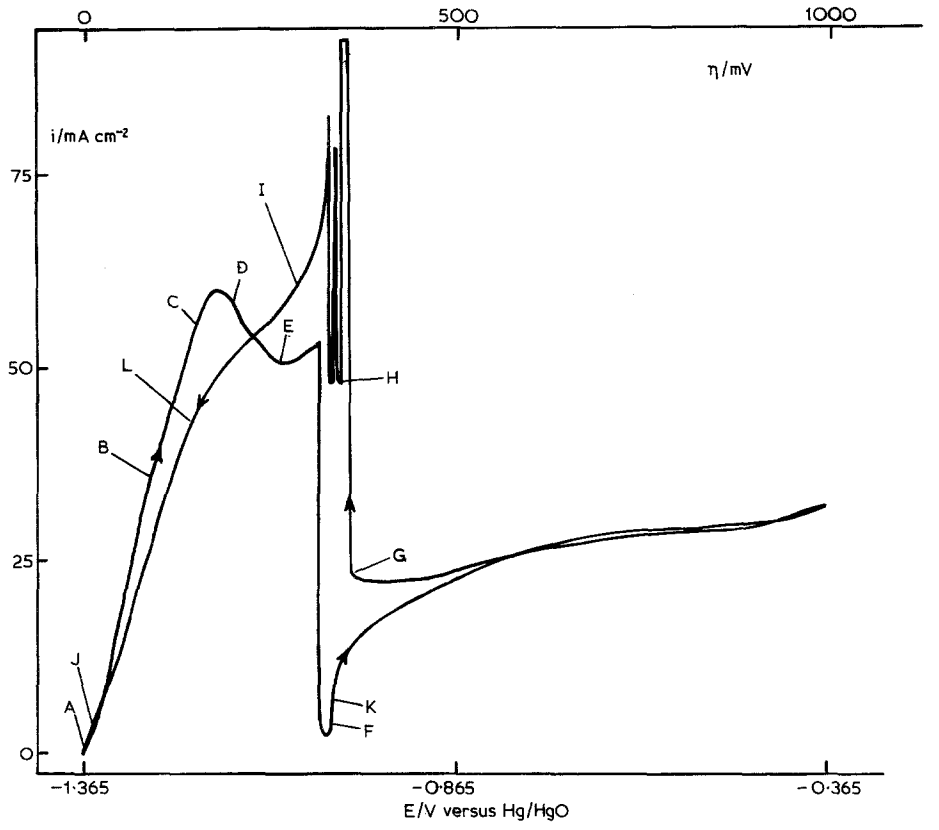

Fig. 6. Cyclic voltammogram for 8 M NaOH/1 M $Na_2Zn(OH)_4$/1 v/o Na_2SiO_3. Sweep rate: 0·83 mV s^{-1}. Non-quiescent electrolyte.

oxide is complicated by the effects of strain energy within the film, the possibility that surface free energies will not be independent of film area and that chemical potentials for substances constituting the monolayer may be different from those of the corresponding bulk solids. A simplified thermodynamic treatment [11] for the case of a circular nucleus, thickness one monolayer, results in the equation

$$\Delta G^* = \frac{\pi a^2 \sigma_{fs}^2}{-a\Delta G_v - (\sigma_{ef} + \sigma_{fs} - \sigma_{es})}, \quad (1)$$

where a is the height of the nucleus, ΔG_v the free energy change per unit volume accompanying the formation of the film, σ_{fs}, σ_{ef} and σ_{es} are the surface free energies of the film-solution, electrode-film and electrode-solution interphases respectively. The overvoltage (η) is included in the term ΔG_v, thus

$$-\Delta G_v = \frac{4{\cdot}2 \cdot 10^7 . nF\rho\eta}{M}, \quad (2)$$

where ρ is the density and M the molecular weight of the film. Provided the composition and texture of the film remained the same, σ_{ef} would be constant; σ_{fs} and σ_{es} would vary because of the variation in composition of the electrolyte but the large decrease in σ_{es} as a consequence of adsorption of silicate ions would presumably eclipse any variation in σ_{fs}. Writing $\sigma_{ef} + \sigma_{fs} - \sigma_{es} = \Delta\sigma$, adsorption would therefore be expected to increase $\Delta\sigma$ with a consequent decrease in the rate of nucleation of the film. The situation would be more complex if the composition and texture of films formed in the presence and absence of silicate ion were to differ; a decrease in ΔG_v concommitant with variation in film composition would appear necessary to explain the observed behaviour.

Although the similar change in slope of the i_m versus $v^{1/2}$ plots when 0·1 and 10 v/o silicate is added suggests that the silicate layer extends into the diffuse region of the double-layer to provide a region of higher viscosity near to the electrode

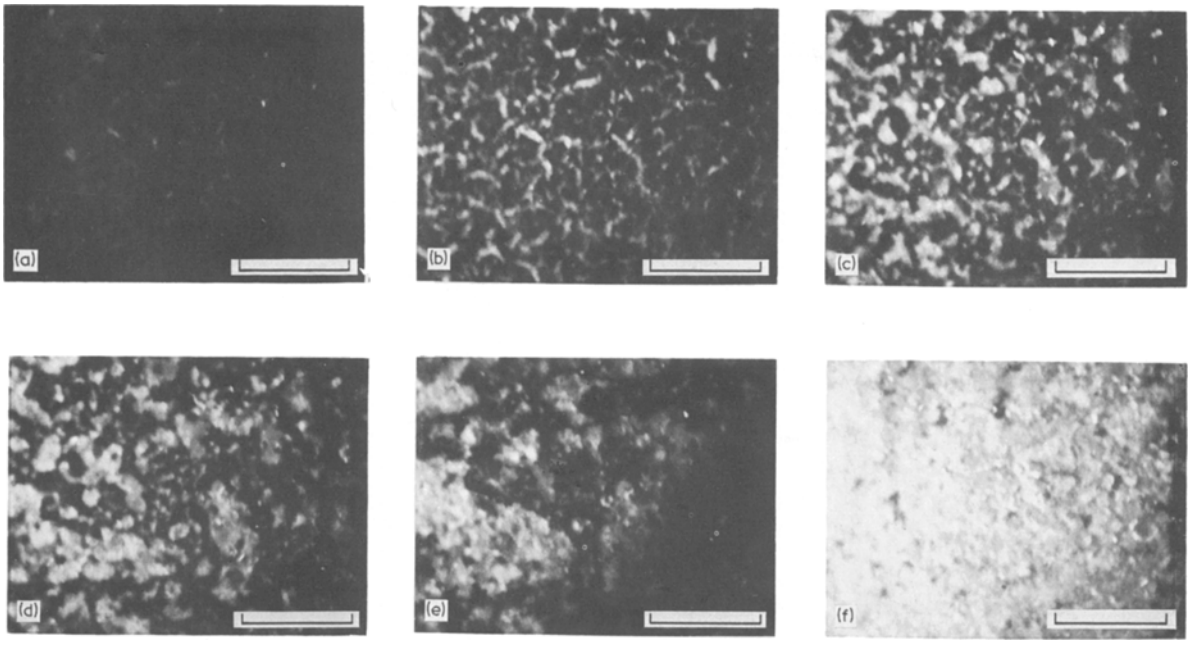

Fig. 7. Optical micrographs of electrode surface. Bar represents 100 μm. Electrolyte: 8 M NaOH/1 v/o Na_2SiO_3.

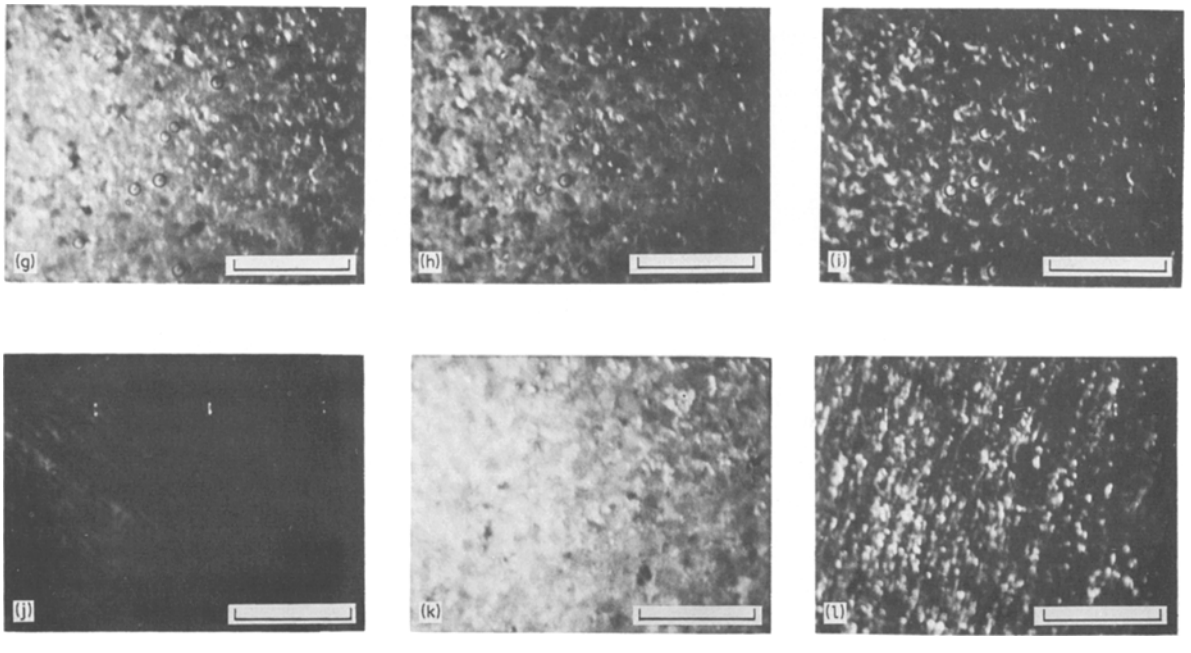

Fig. 8. Optical micrographs of electrode surface. Bar represents 100 μm. Electrolyte: (g, h, i) 8 M NaOH/1 v/o Na_2SiO_3; (j, k, l) 8 M NaOH.

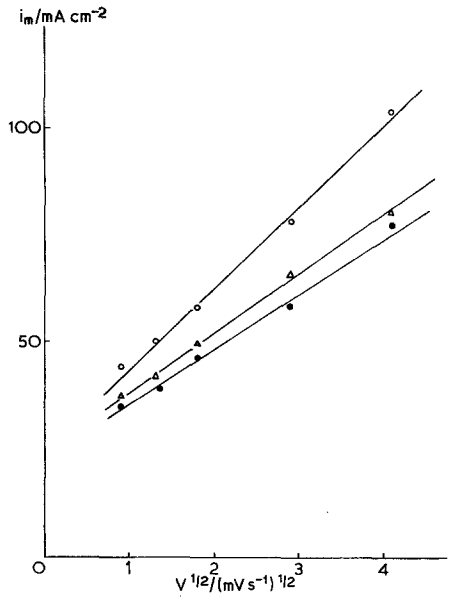

Fig. 9. Sweep rate dependence of i_m. • 10 v/o silicate; △ 1 v/o silicate; ○ no additive.

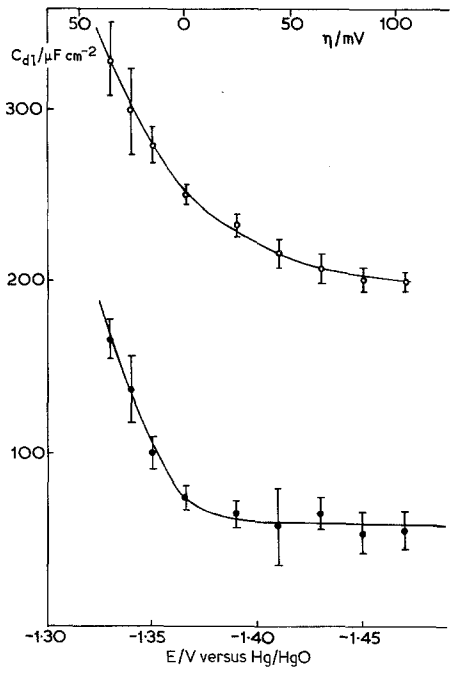

Fig. 10. Potential dependence of double layer capacitance for 8 M NaOH. Bars with ○ – no silicate; bars with • – silicate present.

surface, it is unlikely that this could be responsible for the large cathodic shift of peak I. It is more probable that this displacement arises from the apparent catalytic influence of adsorbed $SiO_3^=$ on the zinc dissolution rate, as a result of which the current density corresponding to saturation within the diffusion layer would be reached earlier in the potential scan. The adsorbed anion presumably influences the kinetics of the reaction by changing the potential of the outer Helmholtz Plane.

The uneven reduction of the film in silicate containing electrolyte probably simply reflects the uneven oxidation as exemplified by the subsidiary peaks in the active-passive transition. The latter were always reproducible and never occurred in the absence of additive. From the micrographs in Fig. 8 it can be seen that the peak preceding point H in the cathodic excursion of Fig. 6 corresponds to partial reduction of the film, which is absent at point I. The uneven oxidation/reduction probably arises from the variation of composition of the film over the electrode surface, as a consequence of the silicate ions adsorbing onto certain preferred sites.

4. Conclusions

Silicate ion although it may act as an extender for the zinc/alkali system by stabilising $ZnO/Zn(OH)_2$ in solution, does not act as a passivation inhibitor in the true sense, i.e. it does not discourage the formation of an oxide film on the zinc surface; despite the presence of an adsorbed film of silicate. Such an additive would be expected to delay the active-passive transition in the anodic potential scan, whereas $SiO_3^=$ apparently has the opposite effect.

References

[1] V.N. Flerov, *Zh. Prikl. Khim.* **30** (1957) 1326.
[2] V.N. Flerov, *ibid* **31** (1957) 49.
[3] V.V. Bakaev, V.N. Shirokov and V.N. Flerov, *Electrokhimiya* **7** (1971) 376.
[4] A. Marshall, N.A. Hampson and J.S. Drury, *J. Electroanal. Chem.* **50** (1974) 292.
[5] R.W. Powers, *Electrochem. Technol.* **5** (1967) 429.
[6] R.W. Powers and M.W. Breiter, *J. Electrochem. Soc.* **116** (1969) 719.
[7] R.W. Powers, *ibid* 1652.
[8] J.J. McMullen and N. Hackerman, *ibid* **106** (1959) 341.
[9] K. Huber, *Helv. Chim. Acta.* **26** (1943) 1037.
[10] K. Huber, *J. Electrochem. Soc.* **100** (1953) 376.
[11] D.A. Vermilyea, Anodic Films. Chapt. IV, Vol III, *Adv. Electrochem.* Eds. P. Delahay and C.W. Tobias, Interscience (1963).